PHYSICAL REVIEW B **91**, 081404(R) (2015)

Optical bistability in electrically driven polariton condensates

M. Amthor,[1] T. C. H. Liew,[2] C. Metzger,[1] S. Brodbeck,[1] L. Worschech,[1] M. Kamp,[1] I. A. Shelykh,[2,3] A. V. Kavokin,[4,5] C. Schneider,[1,6] and S. Höfling[1,7]

[1]*Technische Physik, Wilhelm-Conrad-Röntgen-Research Center for Complex Material Systems, Universität Würzburg, Am Hubland, D-97074 Würzburg, Germany*

[2]*Division of Physics and Applied Physics, Nanyang Technological University, Singapore 637371, Singapore*

[3]*Science Institute, University of Iceland, Dunhagi 3, IS-107 Reykjavik, Iceland*

[4]*Spin Optics Laboratory, St. Petersburg State University, 1, Ulianovskaya, St. Petersburg 198504, Russia*

[5]*Physics and Astronomy School, University of Southampton, Highfield, Southampton SO17 1BJ, United Kingdom*

[6]*Mediterranean Institute of Fundamental Physics, 31, via Appia Nuova, I-00040 Rome, Italy*

[7]*SUPA, School of Physics and Astronomy, University of St. Andrews, St. Andrews KY16 9SS, United Kingdom*

(Received 17 September 2014; revised manuscript received 16 January 2015; published 18 February 2015)

We observe a bistability in an electrically driven polariton condensate, which is manifested by a memory dependent threshold characteristic. In contrast to the polariton bistabilities previously observed in resonantly optically pumped microcavities, our effect occurs under nonresonant electric pumping and is triggered by the current injection scheme. We explain the origin of the bistability by a dependence of the electron-hole tunneling lifetime on the carrier density in the embedded quantum wells. The field screening effect creates a positive feedback loop, which yields the bistable behavior of the condensate. We develop a rate-equation-based model which qualitatively explains the occurrence of the hysteresis under current injection, its reduction with increased magnetic field, and the absence of bistability under optical pumping.

DOI: 10.1103/PhysRevB.91.081404 PACS number(s): 71.36.+c, 71.55.Eq, 73.21.Fg

Introduction. Exciton polaritons evolve in semiconductor microcavities as the result of strong coupling of optical and matter modes [1]. Being low-mass bosons, they manifest quantum coherent properties at temperatures ranging between tens of Kelvin in GaAs and CdTe-based structures [2,3] and room temperature in wide-band-gap materials, such as GaN-based compounds, ZnO, and organic semiconductors [4–7]. Due to polariton condensation, the microcavity becomes a source of coherent emission, which was first predicted in Ref. [8].

Rather conveniently, polariton condensates can be generated optically [2,3], and electrical injection of polaritons in GaAs-based microcavities has also been demonstrated [9,10]. It is in particular the latter scheme which provides an entirely different platform for practical polariton devices, ranging from light sources with low power consumption to electrically controlled integrated circuits.

Such photonic architectures are based on the strong nonlinearities of the quasiparticles inherited from the excitonic part. While the droplets of polariton condensates can propagate over macroscopic distances in designed channel structures [11,12] and two-dimensional systems [13], it is the matter part which allows for the efficient manipulation of the propagating condensate [14–16]. Technological achievements have opened a route to the creation of polariton-based logic elements [17–22] and optical integrated circuits [23,24], which can, in principle, work at relatively high temperatures in wide-band-gap systems. Bistability [25,26] and multistability [27,28] allow for fast [29] and energy efficient switching in such integrated circuit architectures. Furthermore, the inherent memory effect comprised in the hysteresis can be straightforwardly exploited to create a polaritonic memory device as a key ingredient in a logic circuit. The occurrence of conventional bistability in polariton systems is a consequence of the polariton system's huge nonlinearities and the spin degree of freedom acquired by the excitonic component of the quasiparticles. However, to date, bistable effects in polariton systems were only observed under resonant optical injection conditions as an interplay between the density dependent energy shift of the reservoir and the injection efficiency of the pump laser [30], which makes this effect rather cumbersome to implement and difficult to scale. Schemes to achieve bistability in polariton condensates under nonresonant pumping are sought after and predicted [31], based on specially patterned subwavelength grating microcavities [32], yet the experimental demonstration of such an effect is elusive to date. Here, we present evidence for a bistable polariton system operated entirely off resonantly, under electrical injection conditions.

For the description of the observed phenomenon, we exploit a set of standard rate equations, which describe the formation of a polariton condensate from an incoherent electron-hole reservoir, similar to Refs. [1,33]. The difference in our approach, which eventually results in bistability, lies in a feedback mechanism which takes into account an interplay between the persisting electric field of the polariton diode and electrostatic screening. This model explains the occurrence of bistability in our polariton diode under electrical injection, the absence of the effect under nonresonant optical injection, and finally the magnetic field dependency of the hysteresis.

Experimental setup. The sample which we study in this work is similar to the one discussed in Ref. [9]. It is composed of 23(27) doped AlAs/GaAs distributed Bragg reflectors (DBRs) in the bottom (top) mirror. Holes can be injected through the carbon doped top mirror, and electrons through the silicon doped bottom DBR and the *n*-type doped GaAs substrate. The intrinsic λ-thick GaAs Fabry-Pérot cavity spacer contains four InGaAs quantum wells (QWs). Strong coupling conditions are confirmed by photoreflection measurements

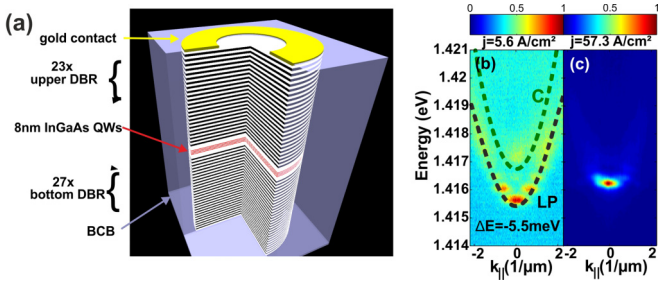

FIG. 1. (Color online) (a) Sketch of the polariton laser diode. (b) Electroluminescence spectrum of the polariton diode recorded at low pumping conditions ($j = 5.6$ A/cm^2). The sample temperature was set to 6 K and a magnetic field of 5 T was applied. The black dashed curve depicts the theoretical dispersion of the lower polariton, while the green dashed curve indicates the bare photon resonance. (c) Dispersion of the electrically injected polariton condensate. The injection current amounts to $j = 57.3$ A/cm^2.

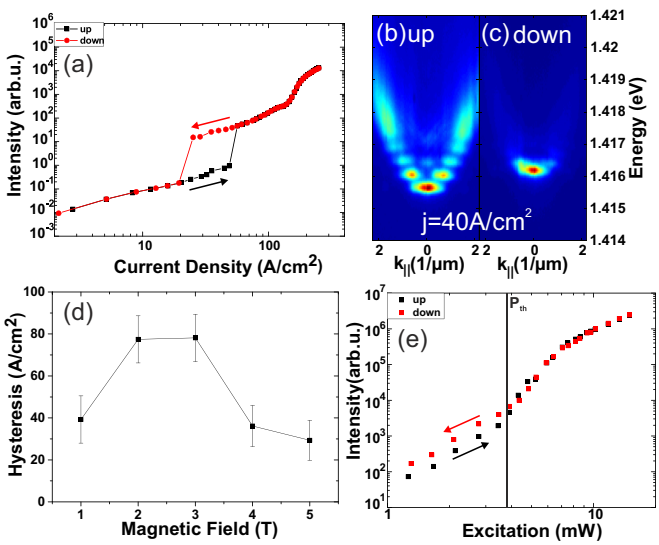

FIG. 2. (Color online) (a) Input-output characteristics of the light emitted from the energy ground state. The polariton laser is characterized by the occurrence of a double threshold. A strong bistability is observed for the first transition from the linear regime to the condensate. (b) Polariton dispersions recorded in the bistable range at a magnetic field of 5 T with increasing pump current, and (c) with decreasing current. (d) Size of the hysteresis as a function of the applied magnetic field. (e) The experiment is repeated for nonresonant optical injection. No hysteresis can be observed in the polariton laser threshold.

and angular resolved electroluminescence for various exciton-photon detuning conditions, and we can extract a Rabi splitting of 5.5 meV (6 meV for a magnetic field of 5 T) [9]. In order to facilitate efficient current injection into the QWs, we etch micropillars with a diameter of 20 μm into the layer structure, which are later planarized by a polymer (benzocyclobuthene), and ring contacts are lithographically defined and evaporated on the top of the pillars. Hence, current can be injected through the ring into the structure without blocking the central emitted signal. Furthermore, the sample can be excited optically with a pump laser. A sketch of the device under investigation is depicted in Fig. 1(a).

Experiment. The formation of a polariton condensate under incoherent electrical injection conditions is evident from the electroluminescence spectra, recorded under continuous wave (cw) conditions shown in Figs. 1(b) and 1(c). The spectra were recorded at a sample temperature of 6 K in a Fourier space setup, which allows us to assess the dispersion characteristics of the emission up to 2 $1/\mu$m. Under moderate pumping conditions ($j = 5.6$ A/cm^2), and at an applied magnetic field of 5 T, the momentum resolved luminescence follows the lower polariton branch [black dashed line, Fig. 1(b)]. The exciton-cavity detuning $\delta = E_c - E_x$ of the chosen device amounts to -5.5 meV, which is on the order of the Rabi splitting. At sufficiently large pumping powers [Fig. 1(c)], the formation of a polariton condensate is indicated by the strong luminescence from the lowest energy state, and the low signal from the excited states. As we show in the Supplemental Material [34], we can clearly resolve a Zeeman splitting in the emission from the ground state in this regime by applying polarization resolved spectroscopy, which proves that strong coupling conditions are preserved.

We will now focus on the power dependence of the luminescence emitted from the polariton ground state. Therefore, we plot the emitted photon flux at zero in-plane momentum as a function of the excitation current in Fig. 2(a). Confirming the observations that we have reported previously [9], we observe a double threshold in the input-output characteristics [35–38], which strongly suggests a crossover from the linear regime to polariton lasing (at $j = 50$ A/cm^2, and a subsequent transition (at $j = 110$ A/cm^2) into the regime of cavity mediated from an electron-hole plasma. It is worth noting that while the second threshold into the weak coupling regime acquires the shape of a smooth S in the double logarithmic plot, the polariton lasing threshold features a sudden increase in intensity. More importantly, we observe a strong modification of the behavior when the injection current is ramped from high to low values. Here, the polariton laser regime can be established over a significantly extended current range, down to a value of $j = 25$ A/cm^2, giving rise to a strongly pronounced bistability in the system. In order to further visualize this effect, we plot both the energy momentum dispersion of the device recorded at an injection current of $j = 40$ A/cm^2, once under increasing current [Fig. 2(b)] and once with decreasing injection current [Fig. 2(c)]. Whereas the dispersion in Fig. 2(b) features all attributes of polaritons in the linear regime, the characteristics in Fig. 2(c) evidence a polariton condensate formation.

This bistability is only observed at the polariton laser related threshold, whereas the second threshold into the weak coupling regime remains completely unaffected by the direction we ramp the injection current. We repeated this experiment under various magnetic fields, and consistently observed bistable behavior over a range between 1 and 5 T. We note that the polariton laser threshold at 0 T cannot be unambiguously determined in the device that we discuss here. We plot the size of the hysteresis loop in terms of the difference between the threshold for polariton lasing with increasing and decreasing injection current [Fig. 2(d)]: A strong dependence of the hysteresis on the magnetic field is observed, with a marked decrease of the size of the hysteresis loop with increasing magnetic field.

We carried out polarization dependent measurements which reveal a degree of linear polarization of 0.08 in the condensate regime. This indicates a different mechanism responsible for the bistability than in electrically driven vertical-cavity surface-emitting lasers (VCSELs) [39]. One could also expect that a mode competition between the Zeeman branches causes the bistability. Therefore, their hysteresis behavior was investigated separately via polarization resolved spectroscopy and no dependence could be found [34]. Additionally, we carried out this experiment under optical pumping conditions. Here, the polaritons were excited by an off-resonant cw laser, which was tuned to the frequency of the first interference minimum of the stop band (approximately 50 meV above the polariton resonance). Polariton condensation is established under these excitation conditions, which is indicated by the nonlinearity in the input-output curve shown in Fig. 2(e). As we have demonstrated elsewhere [40], under optical pumping the system preserves the typical polaritonic properties once this threshold is crossed, such as a notable blueshift of the lasing mode, a consistent linewidth broadening towards higher injection powers, and strong sensitivity to an applied static electric field, which allows us to clearly distinguish this threshold from a conventional photon laser threshold. Although a slightly increased output power is observed for low optical excitation powers during the down sweep, it is important to note that around threshold no notable hysteresis is observed. This behavior is irrespective of the strength of the magnetic field, which strongly suggests that the hysteresis is caused by an effect related to the current injection scheme.

Theory. In order to explain the observed behavior, we solve the polariton rate equations which govern our nonresonantly driven system. Polariton condensation is achieved under electrical injection via the initial population of charged carriers (electrons and holes), which relax into quantum well excitons and finally condense into polaritons. The corresponding rates of exciton formation (W_1), dissociation (W_2), and condensation $r(n_p+1)$ are illustrated in Fig. 3(a), together with the decay rates for charged carriers (γ), excitons (γ_x), and polaritons (γ_p). While we will assume the parameters $W_{1,2}$, r, and γ_p to be constant, we will later account for a nonlinear dependence of γ on the carrier density n as a result of electrostatic screening. Additionally, the exciton decay rate acquires a dependency on the magnetic field B, since the oscillator strength increases with B.

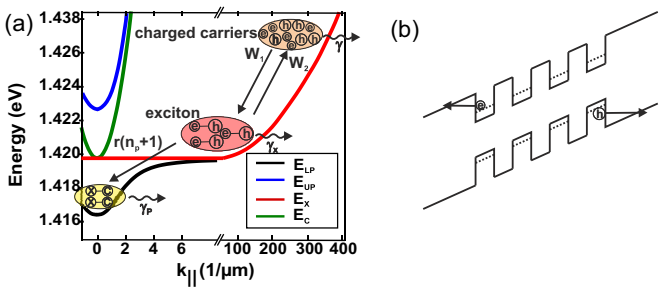

FIG. 3. (Color online) (a) Illustration of processes leading to polariton condensation under electrical injection. (b) Driving of electrons and holes out of the system by the applied electric field, resulting in the decay γ.

Assuming a spatially homogeneous excitation, the numbers of charged carriers (n), excitons (n_x), and polaritons (n_p) in the micropillar evolve according to the coupled rate equations:

$$\frac{\partial n}{\partial t} = P - W_1 n^2 + W_2 n_x - \gamma n, \tag{1}$$

$$\frac{\partial n_x}{\partial t} = W_1 n^2 - W_2 n_x - \gamma_x n_x - r(n_p+1)n_x, \tag{2}$$

$$\frac{\partial n_p}{\partial t} = r(n_p+1)n_x - \gamma_p n_p. \tag{3}$$

We have assumed that the electron and hole populations are similar, being described by a single pumping rate P, corresponding to the application of an electric field across the quantum wells. The electric field is also responsible for driving the free carriers out of the structure, corresponding to the decay rate γ [see Fig. 3(b)]. Typically the decay rate grows exponentially with the electric field [41]. However, since we operate our diode in the forward direction, the dependency of the internal electric field on the applied voltage is modest. Nevertheless, as we inject more carriers into the active region, a persisting internal field can be further decreased due to the screening of the electric field by free carriers. This results in a decrease of the carrier decay rate with increasing bias,

$$\gamma = \gamma_0 e^{-cn}, \tag{4}$$

where γ_0 and c are constants. The steady-state solution to Eqs. (1)–(3) is

$$P = W_1 n^2 - W_2 n_x + \gamma_0 e^{-cn} n, \tag{5}$$

$$n = \sqrt{\frac{n_x}{W_1}[W_2 + \gamma_x + r(n_p+1)]}, \tag{6}$$

$$n_p = \frac{r n_x}{\gamma_p - r n_x}. \tag{7}$$

The reduction of the loss rate γ upon increasing the carrier density n generates a positive feedback which is sufficiently strong to cause bistability in our system. This is evident in Fig. 4(a), where we plot the polariton number n_p as a function of the pump power P, obtained from Eqs. (5)–(7). Qualitatively similar hysteresis behavior is also obtained with different forms of the introduced nonlinearity. As we show in the Supplemental Material [34], bistability is also present when n enters Eq. (4) with a quadratic or square root dependence in the exponent.

As we have shown above in Fig. 2(e), the hysteresis is absent under nonresonant optical pumping. The localized excitation of electrons and holes leads to a significantly faster exciton formation and therefore reduces the free carrier density. Being electrically neutral, excitons contribute very little to the screening of the external electric field. This is why the bistability is only seen in the case of electrical injection. This behavior is confirmed by our theory, as we take $\gamma = 0$ in the absence of an applied electric field and replace the quantity $W_1 n^2 - W_2 n_x$ in Eq. (2) with P (which now represents the exciton pumping rate). The according curves are plotted as dashed lines in Fig. 4(a).

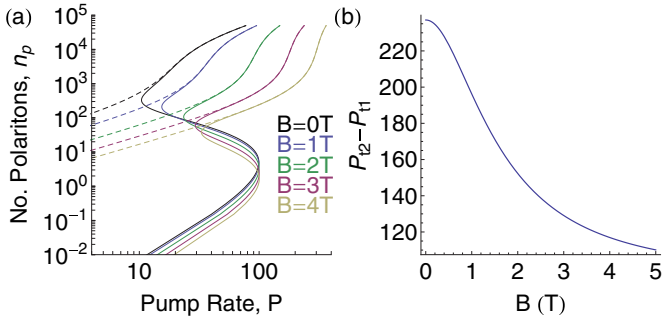

FIG. 4. (Color online) (a) Power dependence of the polariton number, for different magnetic field strengths. Solid curves show results under electrical injection, where γ is defined by Eq. (4); dashed curves show results under optical injection, where $\gamma = 0$. (b) Dependence of the width of the hysteresis zone on the magnetic field. Parameters: $r = 10^{-3}$ ps^{-1}, $W_1 = 1.5 \times 10^{-5}$ ps^{-1}, $W_2 = 0.2$ ps^{-1}, $\gamma_0 = 0.3$ ps^{-1}, $\gamma_{x,0} = 0.03$ ps^{-1}, $\gamma_p = 1/15$ ps^{-1}, $B_1 = 1$ T, $c = 0.01$ ps^{-1}.

We can also account for different magnetic field strengths in the system in our model. With increasing magnetic field, the exciton decay rate is expected to increase [42]:

$$\gamma_x = \gamma_{x,0}\left(1 + \frac{B^2}{B_1^2}\right). \tag{8}$$

Consequently, this additional loss channel weakens the influence of the nonlinearity generated by the feedback between pumping and screening, and the effect is continuously smeared out. This is directly reflected in the width of the hysteresis region, which successively decreases for increasing magnetic fields, as shown in Fig. 4(b). While this is in qualitative agreement with the experimentally observed behavior for large magnetic fields >2 T, the additional, nonmonotonous behavior observed experimentally may be due to the magnetic field dependence of carrier diffusion rates. Accounting for this effect would require a description of the spatial degrees of freedom, which is beyond the scope of this Rapid Communication.

Conclusion. We observed optical bistability in an electrically driven polariton laser. This demonstration of bistability in polariton lasers under electric injection is explained in terms of an interplay between the tunneling lifetime of the electron-hole reservoir and electrostatic screening, which causes a positive feedback loop under electrical injection, leading to strong hysteresis. This work opens up a route towards hybrid electro-optic polaritonic devices, where coherent optical signals are injected electrically and memory elements in polaritonic integrated circuits.

The authors would like to thank the State of Bavaria for financial support. We thank M. Lermer and A. Wolf for support in sample fabrication. Furthermore, we thank A. Rahimi-Iman for initial characterizations and discussions. I.A.S. acknowledges the support of FP7 IRSES project POLAPHEN. S.H. gratefully acknowledges support by the Royal Society and the Wolfson Foundation. A.V.K. acknowledges financial support from the Ministry of Education and Science of the Russian Federation (Contract No. 11.G34.31.0067 with SPbSU), and EU projects POLAPHEN, SPANGL4Q, and LIMACONA. We thank I.G. Savenko, Ö. Bozat, and H. Flayac for discussions.

[1] A. Kavokin, J. Baumberg, G. Malpuech, and F. Laussy, *Microcavities* (Clarendon, Oxford, U.K., 2006).
[2] J. Kasprzak, M. Richard, S. Kundermann, A. Baas, P. Jeambrun, J. M. J. Keeling, F. M. Marchetti, M. H. Szymanska, R. André, J. L. Staehli, V. Savona, P. B. Littlewood, B. Deveaud, and L. S. Dang, Nature (London) **443**, 409 (2006).
[3] R. Balili, V. Hartwell, D. Snoke, L. Pfeiffer, and K. West, Science **316**, 1007 (2007).
[4] S. Christopoulos, G. Baldassarri Höger von Högersthal, A. J. D. Grundy, P. G. Lagoudakis, A. V. Kavokin, J. J. Baumberg, G. Christmann, R. Butté, E. Feltin, J.-F. Carlin, and N. Grandjean, Phys. Rev. Lett. **98**, 126405 (2007).
[5] T.-C. Lu, Y.-Y. Lai, Y.-P. Lan, S.-W. Huang, J.-R. Chen, Y.-C. Wu, W.-F. Hsieh, and H. Deng, Opt. Express **20**, 5530 (2012).
[6] J. D. Plumhof, T. Stöferle, L. Mai, U. Scherf, and R. F. Mahrt, Nat. Mater. **13**, 248 (2014).
[7] K. S. Daskalakis, S. A. Maier, R. Murray, and S. Kéna-Cohen, Nat. Mater. **13**, 272 (2014).
[8] A. Imamoglu, R. J. Ram, S. Pau, and Y. Yamamoto, Phys. Rev. A **53**, 4250 (1996).
[9] C. Schneider, A. Rahimi-Iman, N. Y. Kim, J. Fischer, I. G. Savenko, M. Amthor, M. Lermer, A. Wolf, L. Worschech, V. D. Kulakovskii, I. A. Shelykh, M. Kamp, S. Reitzenstein, A. Forchel, Y. Yamamoto, and S. Höfling, Nature (London) **497**, 348 (2013).
[10] P. Bhattacharya, B. Xiao, A. Das, S. Bhowmick, and J. Heo, Phys. Rev. Lett. **110**, 206403 (2013).
[11] J. Fischer, I. G. Savenko, M. D. Fraser, S. Holzinger, S. Brodbeck, M. Kamp, I. A. Shelykh, C. Schneider, and S. Höfling, Phys. Rev. Lett. **113**, 203902 (2014).
[12] E. Wertz, L. Ferrier, D. D. Solnyshkov, R. Johne, D. Sanvitto, A. Lemaître, I. Sagnes, R. Grousson, A. V. Kavokin, P. Senellart, G. Malpuech, and J. Bloch, Nat. Phys. **6**, 860 (2010).
[13] B. Nelsen, G. Liu, M. Steger, D. W. Snoke, R. Balili, K. West, and L. Pfeiffer, Phys. Rev. X **3**, 041015 (2013).
[14] T. Gao, P. S. Eldridge, T. C. H. Liew, S. I. Tsintzos, G. Stavrinidis, G. Deligeorgis, Z. Hatzopoulos, and P. G. Savvidis, Phys. Rev. B **85**, 235102 (2012).
[15] G. Tosi, G. Christmann, N. G. Berloff, P. Tsotsis, T. Gao, Z. Hatzopoulos, P. G. Savvidis, and J. J. Baumberg, Nat. Phys. **8**, 190 (2012).
[16] H. S. Nguyen, D. Vishnevsky, C. Sturm, D. Tanese, D. Solnyshkov, E. Galopin, A. Lemaître, I. Sagnes, A. Amo, G. Malpuech, and J. Bloch, Phys. Rev. Lett. **110**, 236601 (2013).
[17] T. C. H. Liew, A. V. Kavokin, and I. A. Shelykh, Phys. Rev. Lett. **101**, 016402 (2008).
[18] A. Amo, T. C. H. Liew, C. Adrados, R. Houdré, E. Giacobino, A. V. Kavokin, and A. Bramati, Nat. Photonics **4**, 361 (2010).
[19] C. Adrados, T. C. H. Liew, A. Amo, M. D. Martin, D. Sanvitto, C. Antón, E. Giacobino, A. Kavokin, A. Bramati, and L. Viña, Phys. Rev. Lett. **107**, 146402 (2011).

[20] M. De Giorgi, D. Ballarini, E. Cancellieri, F. M. Marchetti, M. H. Szymanska, C. Tejedor, R. Cingolani, E. Giacobino, A. Bramati, G. Gigli, and D. Sanvitto, Phys. Rev. Lett. **109**, 266407 (2012).
[21] M. Steger, C. Gautham, B. Nelsen, D. Snoke, L. Pfeiffer, and K. West, Appl. Phys. Lett. **101**, 131104 (2012).
[22] D. Ballarini, M. De Giorgi, E. Cancellieri, R. Houdre, E. Giacobino, R. Cingolani, A. Bramati, G. Gigli, and D. Sanvitto, Nat. Commun. **4**, 1778 (2013).
[23] T. C. H. Liew, A. V. Kavokin, T. Ostatnicky, M. Kaliteevski, I. A. Shelykh, and R. A. Abram, Phys. Rev. B **82**, 033302 (2010).
[24] T. Espinosa-Ortega and T. C. H. Liew, Phys. Rev. B **87**, 195305 (2013).
[25] A. Baas, J. P. Karr, H. Eleuch, and E. Giacobino, Phys. Rev. A **69**, 023809 (2004).
[26] D. Bajoni, E. Semenova, A. Lemaître, S. Bouchoule, E. Wertz, P. Senellart, S. Barbay, R. Kuszelewicz, and J. Bloch, Phys. Rev. Lett. **101**, 266402 (2008).
[27] N. A. Gippius, I. A. Shelykh, D. D. Solnyshkov, S. S. Gavrilov, Y. G. Rubo, A. V. Kavokin, S. G. Tikhodeev, and G. Malpuech, Phys. Rev. Lett. **98**, 236401 (2007).
[28] T. K. Paraïso, M. Wouters, Y. Leger, F. Morier-Genoud, and B. Deveaud-Plédran, Nat. Mater. **9**, 655 (2010).
[29] R. Cerna, Y. Léger, T. Paraïso, M. Wouters, F. Morier-Genoud, M. T. Portella-Oberli, and B. Deveaud, Nat. Commun. **4**, 2008 (2013).
[30] S. S. Gavrilov, A. V. Sekretenko, N. A. Gippius, C. Schneider, S. Höfling, M. Kamp, A. Forchel, and V. D. Kulakovskii, Phys. Rev. B **87**, 201303 (2013).
[31] O. Kyriienko, E. A. Ostrovskaya, O. A. Egorov, I. A. Shelykh, and T. C. H. Liew, Phys. Rev. B **90**, 125407 (2014).
[32] B. Zhang, Z. Wang, S. Brodbeck, C. Schneider, M. Kamp, S. Höfling, and H. Deng, Light: Sci. Appl. **3**, e135 (2014).
[33] I. Iorsh, M. Glauser, G. Rossbach, J. Levrat, M. Cobet, R. Butté, N. Grandjean, M. A. Kaliteevski, R. A. Abram, and A. V. Kavokin, Phys. Rev. B **86**, 125308 (2012).
[34] See Supplemental Material at http://link.aps.org/supplemental/10.1103/PhysRevB.91.081404 for further details.
[35] L. S. Dang, D. Heger, R. André, F. Bœuf, and R. Romestain, Phys. Rev. Lett. **81**, 3920 (1998).
[36] D. Bajoni, P. Senellart, E. Wertz, I. Sagnes, A. Miard, A. Lemaître, and J. Bloch, Phys. Rev. Lett. **100**, 047401 (2008).
[37] B. Nelsen, R. Balili, D. W. Snoke, L. Pfeiffer, and K. West, J. Appl. Phys. **105**, 122414 (2009).
[38] J.-S. Tempel, F. Veit, M. Aßmann, L. E. Kreilkamp, A. Rahimi-Iman, A. Löffler, S. Höfling, S. Reitzenstein, L. Worschech, A. Forchel, and M. Bayer, Phys. Rev. B **85**, 075318 (2012).
[39] H. Kawaguchi, IEEE J. Sel. Top. Quantum Electron. **3**, 1254 (1997).
[40] M. Amthor, S. Weißenseel, J. Fischer, M. Kamp, C. Schneider, and S. Höfling, Opt. Express **22**, 31146 (2014).
[41] K. Sivalertporn, L. Mouchliadis, A. L. Ivanov, R. Philp, and E. A. Muljarov, Phys. Rev. B **85**, 045207 (2012).
[42] S. N. Walck and T. L. Reinecke, Phys. Rev. B **57**, 9088 (1998).